

O-TRENTOX, a New Tripodal Iron Chelator Based on 8-Hydroxyquinoline Subunits: Thermodynamic and Kinetic Studies

Guy Serratrice,* Hakim Boukhalfa, Claude Béguin, Paul Baret, Catherine Caris, and Jean-Louis Pierre

Laboratoire de Chimie Biomimétique, LEDSS, UMR CNRS No. 5616, Université Joseph Fourier, BP 53, Grenoble Cedex 9, France

Received July 10, 1996[⊗]

The thermodynamic stability of Fe(III) complexes with a new hexadentate tripodal ligand (O-TRENTOX) incorporating three 8-hydroxyquinoline (“oxine”) subunits, linked to a tetraamine (“TREN”) via an amide connection, has been investigated by the use of UV–vis spectrophotometry and potentiometric methods. O-TRENTOX has been found to form, at pH < 1, a protonated complex FeLH₅²⁺ (orange color) which deprotonates, over the pH range 1–2, to a green complex FeLH₂²⁻ through a four-proton process. The first protonation constant of ferric O-TRENTOX has been determined to be 5.60. The stability constant log β₁₁₀ has been determined to be 30.9. A pFe (pFe = –log [Fe³⁺]) value of 29.5 has been calculated at pH = 7.4, [ligand]_{tot} = 10 μM, and [Fe³⁺]_{tot} = 1 μM, indicating that O-TRENTOX is one of the most powerful among the iron synthetic chelators. Cyclic voltammetry experiments have shown that the system Fe^{III}–O-TRENTOX/Fe^{II}–O-TRENTOX is quasi reversible, with a redox potential of 0.087 V vs NHE. This value is related to the high complexing ability of O-TRENTOX for both the ferric and ferrous iron redox states, making it relevant for biological uses. The kinetics of formation and acid hydrolysis of the ferric O-TRENTOX complex have been investigated in acidic medium using the diode array stopped-flow spectrophotometry technique in 2.0 M NaClO₄/HClO₄ at 25 °C. The determining step for the complex formation involves the reaction of FeOH²⁺ with the LH₇⁺ ligand species, with a rate constant of 789 ± 17 M⁻¹ s⁻¹. The acid hydrolysis of the FeLH₂²⁻ complex in 0.02–1.0 M HClO₄ and ionic strength 2.0 M NaClO₄/HClO₄ leads to the FeLH₅²⁺ complex, indicating that O-TRENTOX is a very strong chelating agent for Fe(III) in acidic medium. The kinetic data have been interpreted by a stepwise mechanism related to the successive protonation of four binding sites. The spectroscopic change is consistent with removal of one arm of the ligand followed by a shift from a bis(oxinate) to a bis(salicylate) mode of coordination.

Introduction

Although iron is one of the most common elements on Earth, its availability to living organisms is limited because of its extremely low solubility.¹ In response to this challenge, many microorganisms secrete low-molecular-weight chelating agents (siderophores) that possess a high affinity for iron(III). These ligands make soluble ferric iron and facilitate its transport from the extracellular medium into the cells.^{2–5} Siderophores typically contain hydroxamate or catecholate groups to bind the ferric ion, giving octahedral complexes. On the other hand, plants develop different strategies for enhancing iron uptake, one of them using phytosiderophores,⁶ such as mugineic acid that possesses two amino acid groups and one hydroxy acid group.⁷ Nevertheless, plants can develop syndromes of iron deficiency such as iron chlorosis, especially in calcareous soils, and diminishing this problem is fundamentally important for

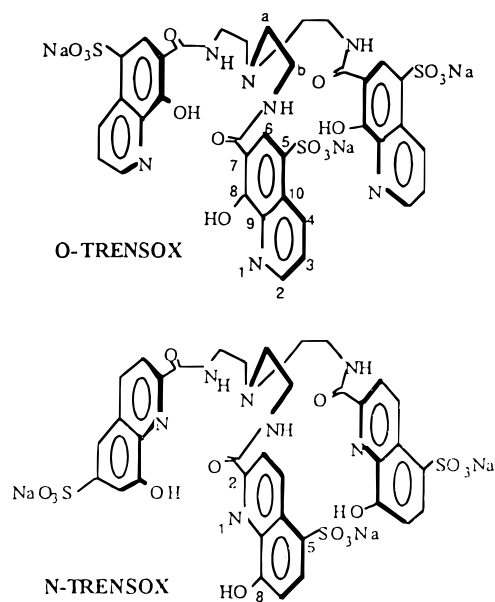
higher food production. Furthermore, iron overload is a common and serious disease which needs iron chelation therapy.⁸ The methanesulfonate of desferrioxamine B (Desferal), a natural trihydroxamate siderophore, is currently used as a drug for the treatment of iron overload.^{1,4} The use of Desferal suffers a number of limitations (it requires subcutaneous administration, short duration of action, prohibitive price), and an important part of the research on iron chelation is focused on the development of orally more effective drugs. Several authors have developed strategies of synthesis of chelating agents which could mimic natural siderophores i.e. which contain hydroxamate and/or catechol groups. The most important work was carried out by the group of Raymond, who has described numerous tricatecholate ligands.^{3,4,9,10} Several series of trihydroxamate ligands have also been synthesized.^{11–15} Recently, octadentate desferrioxamine B catechol derivatives have been prepared.¹⁶ These derivatives have been shown to be more effective iron(III) chelators at pH 7.4 than their parent

[⊗] Abstract published in *Advance ACS Abstracts*, August 1, 1997.

- (1) Crichton, R. R. *Inorganic Biochemistry of Iron Metabolism*; Ellis Horwood: Chichester, U.K., 1991.
- (2) Neilands, J. B. *Struct. Bonding* **1984**, 58, 1–25.
- (3) Raymond, K. N.; Müller, G.; Matzanke, B. F. *Top. Curr. Chem.* **1984**, 123, 49–102.
- (4) Matzanke, B. F.; Müller-Matzanke, G.; Raymond, K. N. *Iron Carriers and Iron Proteins, Physical Bioinorganic Chemistry Series*; Loehr, T. M., Ed.; VCH Publishers: New York, 1989; Vol. 5, pp 1–121.
- (5) Winkelmann, G. *Handbook of Microbial Iron Chelates*; Winkelmann, G., Ed.; CRC Press: Boca Raton, FL 1991; pp 15–64.
- (6) Römhild, V. *Iron Transport in Microbes, Plants and Animals*; Winkelmann, G., Van der Helm, D., Neilands, J. B., Eds; VCH Publishers: Weinheim, Germany, 1987; pp 353–374.
- (7) Sugiura, Y.; Tanaka, H.; Mino, Y.; Ishida, T.; Ota, N.; Inoue, M.; Nomoto, K.; Yoshioka, H.; Takemoto, T. *J. Am. Chem. Soc.* **1981**, 103, 6979–6982.

- (8) Dobbin, P. S.; Hider, R. C. *Chem. Br.* **1990**, 565–568.
- (9) Rodgers, S. J.; Lee, C. W.; Ng, C. Y.; Raymond, K. N. *Inorg. Chem.* **1987**, 26, 1622–1625.
- (10) Stack, T. D. P.; Hou, Z.; Raymond, K. N. *J. Am. Chem. Soc.* **1993**, 115, 6466–6467.
- (11) Sun, Y.; Martell, A. E.; Motekaitis, R. J. *Inorg. Chem.* **1988**, 24, 4343–4350.
- (12) Motekaitis, R. J.; Sun, J.; Martell, A. E. *Inorg. Chem.* **1991**, 30, 1554–1556.
- (13) Shanzer, A.; Libman, J.; Lazar, R.; Tor, Y. *Pure Appl. Chem.* **1989**, 61, 1529–1534.
- (14) Ng, C. Y.; Rodgers, S. J.; Raymond, K. N. *Inorg. Chem.* **1989**, 28, 2062–2066.
- (15) Yakirevitch, P.; Rochel, N.; Albrecht-Gary, A. M.; Libman, J.; Shanzer, A. *Inorg. Chem.* **1993**, 32, 1779–1787.

compound. Some ligands possess a tripodal structure based on the backbone of tris(2-aminoethyl)amine (TREN). This central organizing unit ("spacer") is connected through a trisamide moiety to pendant arms each containing a bidentate group such as catechol,⁹ hydroxamate,¹⁴ or 2,2'-dihydroxybiphenyl.¹⁷ However, no ligand containing 8-hydroxyquinoline subunits has been described. The synthetic 8-hydroxyquinoline (oxine) is a well-known complexing agent used in analytical chemistry, but few studies appear in the literature concerning complexation of Fe(III).¹⁸ Furthermore, 8-hydroxyquinoline-5-sulfonic acid (sulfoxine) forms water-soluble ferric complexes and is a good chelating agent.^{19,20} This stimulated us to investigate a new series of siderophores analogs based on the TREN spacer and related to sulfoxine subunits for water solubility. Two ligands were synthesized by connecting the TREN backbone through a trisamide moiety to the 2-position or the 7-position of sulfoxine. The structures of the two derivatives (named N-TRENSEX and O-TRENSEX, respectively) are depicted as follows:



A preliminary report on the properties of the ferric O-TRENSEX complex has been published.²¹ The ferric complex exhibits highly promising properties for plant nutrition,²² and the free ligand seems to be well-suited for iron chelation therapy.²³ In this article we present a detailed investigation of this ligand and its Fe(III) complexes in aqueous solution, including potentiometric, spectroscopic, and electrochemical studies. The ligand N-TRENSEX was not studied extensively, but some results are described for comparison with O-TRENSEX. Kinetic studies were carried out in order to assess the mechanism of iron complexation and release. In particular, the

spectroscopic study of the complexation of ferric ion by O-TRENSEX has provided evidence of a change from a bis(salicylate) to a bis(oxinate) mode of coordination on raising the pH. So, the kinetic study of the protonation of the ferric O-TRENSEX complex using the pH jump method provides kinetic evidence of a process involving a change in the coordination environment of the ferric ion.

Experimental Section

Materials. All the commercial reagents were of the highest purity and were used without further purification. Iron(III) stock solutions were prepared by dissolving appropriate amounts of ferric perchlorate hydrate (Aldrich) in standardized HClO₄, NaClO₄ solutions. The solutions were standardized for ferric ion spectrophotometrically by using a molar extinction coefficient of 4160 M⁻¹ cm⁻¹ at 240 nm.²⁴ The syntheses of the unsulfonated analogues of N-TRENSEX and O-TRENSEX have been described elsewhere.²⁵ The sulfonated derivatives were prepared according to the method earlier described.²¹

Potentiometric and Spectrophotometric Experiments. All the measurements were made at 25 °C, and the solutions were prepared with deionized and bidistilled water. The ionic strength was fixed at 0.1 M with sodium perchlorate (PROLABO puriss). The pH measurements were performed using a TACUSSEL Ionoprocasseur-II millivoltmeter equipped with glass and calomel electrodes (TACUSSEL). The electrodes were calibrated to read p[H] according to the classical method.²⁶ Potentiometric titration employed a TACUSSEL buret Electrobox and a pH meter (Ionoprocasseur-II) connected to a Hewlett Packard microcomputer. The automation of the titration was realized using software developed in our laboratory. The ligands and their iron(III) complexes of ca. 0.001 M were titrated with standardized 0.05 M sodium hydroxide 0.05. The titration data were refined by the nonlinear least-squares refinement program SUPERQUAD²⁷ to determine the equilibrium constants (protonation and complexation).

Electronic absorption spectra were recorded on a Perkin-Elmer Lambda 2 spectrometer using 1.000 cm path length quartz cells and connected to a COMPACQ Despro 386 s microcomputer. The ferric complexes were investigated in two sets of experimental conditions. (i) The UV-visible spectra of solutions containing Fe(III) in excess with respect to the ligand were recorded for various H⁺ concentrations: the ligand concentration was constant (10⁻⁴ M), and the Fe(III) concentrations were 10⁻³–10⁻⁴ M (5–8 values) for each H⁺ concentration (5 values from 0.3 to 1.5 M HClO₄ standardized solutions). The H⁺ produced by hydrolysis and dimerization of Fe(III) was assumed to be negligible. (ii) The UV-visible spectra of a solution containing equal amounts of ligand and Fe(III) (10⁻⁴ M) were monitored as a function of pH over the range 1–10 (adjusted with HClO₄ or NaOH). An aliquot was taken from the solution after each adjustment of the pH (which was measured using a pHmeter) and its spectrum recorded. The ionic strength was fixed at 0.1 M with NaClO₄/HClO₄ for this second set of experiments. The spectrophotometric data were fitted with the LETAGROP-SPEFO program.²⁸ The program uses a nonlinear least-squares method and calculates the thermodynamic constants of the absorbing species and their corresponding electronic spectra. The calculations were done from absorbances data of about 8–10 wavelength (between 400 and 650 nm).

The spectrophotometric competition was carried out with Na₂H₂-EDTA over the pH range 2–3. Typical solutions were 10⁻⁴ M in ferric ion and ligand with up to a 2-fold excess of Na₂H₂EDTA. The samples were allowed to equilibrate for 72 h at 25 °C.

Spectrometry. Infrared spectra were recorded on a Magna-IR 550 Nicolet spectrometer. Samples were run as KBr pellets. ¹H and ¹³C NMR spectra were recorded on AM 400 Bruker apparatus working at

- (16) Hou, Z.; Whisenhunt, D. W.; Raymond, K. N. *J. Am. Chem. Soc.* **1994**, *116*, 840–846.
 (17) Serratrice, G.; Moural, C.; Zeghli, A.; Béguin, C. G.; Baret, P.; Pierre, J.-L. *New J. Chem.* **1994**, *18*, 749–758.
 (18) Turnquist, T. D.; Sandell, E. B. *Anal. Chim. Acta* **1968**, *42*, 239–245.
 (19) Richard, C. F.; Gustafson, R. L.; Martell, A. E. *J. Am. Chem. Soc.* **1959**, *81*, 1033–1040.
 (20) Gerard, C.; Chehhal, H.; Hugel, R. P. *Polyhedron* **1994**, *13*, 591–597.
 (21) Baret, P.; Béguin, C. G.; Boukhalfa, H.; Caris, C.; Laulhère, J.-P.; Pierre, J.-L.; Serratrice, G. *J. Am. Chem. Soc.* **1995**, *117*, 9760–9761.
 (22) Caris, C.; Baret, P.; Béguin, C. G.; Serratrice, G.; Pierre, J.-L.; Laulhère, J.-P. *Biochem. J.* **1995**, *312*, 879–885.
 (23) Lescoat, G.; Chenoufi, N.; Zanninelli, G.; Loreal, O.; Padeloup, N.; Brissot, P.; Caris, C.; Baret, P.; Pierre, J.-L. *Hepatology (St. Louis)* **1994**, *20*, 182A.

- (24) Bastian, R.; Weberling, R.; Palilla, F. *Anal. Chem.* **1956**, *28*, 459–462.
 (25) Caris, C.; Baret, P.; Pierre, J.-L.; Serratrice, G. *Tetrahedron* **1996**, *52*, 4659–4672.
 (26) Martell, A. E.; Motekaitis, R. J. *Determination and use of stability constants*, 2nd ed.; VCH Publishers: New York, 1992.
 (27) Gans, P.; Sabatini, A.; Vacca, A. *J. Chem. Soc., Dalton Trans.* **1985**, 1195–1200.
 (28) Sillen, L. G.; Warsquist, B. *Arkiv. Kemi* **1968**, *31*, 377–390.

400.13 MHz for ^1H and 100.62 MHz for ^{13}C . The pyridine ring proton signals were assigned on the basis of the coupling constants $^3J(\text{H}-3, \text{H}-4)$ larger than $^3J(\text{H}-2, \text{H}-3)$.²⁹ The more deshielded methylene signal correspond to the one bonded to the NH amide. The ^{13}C signals were assigned using a heteronuclear $^1\text{H}-^{13}\text{C}$ shift correlation. 2D experiments were performed using standard sequences.

Electrochemistry. The electrochemical behavior of the Fe–O-TRENSEX redox system was studied in aqueous media using 0.1 M NaClO_4 as supporting electrolyte by starting from either the ferrous or the ferric complex. The ferrous O-TRENSEX complex was prepared in deoxygenated aqueous solution using FeSO_4 (Aldrich) and was characterized by its UV–visible spectrum²¹ (band at 576 nm, $\epsilon = 1700 \text{ M}^{-1}\text{cm}^{-1}$ at pH 7.5). The pH was adjusted with a diluted aqueous solution of NaOH or HClO_4 . Experiments were carried out using a PAR Model 273 potentiostat. The electrochemical curves were recorded on a Kipp-Zonen x-y recorder. All experiments were run under an argon atmosphere at room temperature. A standard three-electrode electrochemical cell was used. The working electrode was a platinum disk electrode (diameter 5 mm) polished with $2 \mu\text{m}$ diamond paste. When NaClO_4 is employed as the supporting electrolyte, it is advisable to replace the reference electrode solution with NaCl solution in order to avoid the formation of solid KClO_4 in the liquid junction. Experiments were carried out using either an Ag/AgCl , KCl saturated reference electrode or Ag/AgCl , NaCl saturated reference electrode, and very similar results have been found using these two reference electrodes. Potentials referenced to the Ag/AgCl system can be converted into the NHE by adding 0.197 V (KCl saturated) or 0.204 V (NaCl saturated).

Kinetic Studies. Kinetic measurements were performed with a KINSPEC UV (BIO-LOGIC Co., Echirrolles, France) stopped-flow spectrophotometer equipped with a diode array detector (J & M) and connected to a TANDON microcomputer. The kinetic data were treated on line with the commercial BIO-KINE program (BIO-LOGIC Co., Claix, France). The ionic strength was fixed at 2 M (NaClO_4 , HClO_4) owing to the H^+ concentrations up to 1 M and to allow comparisons with literature data.

Formation kinetics were carried out under pseudo-first-order conditions at 25 °C with Fe(III) in excess with respect to the ligand. The Fe(III) concentration was varied from 2×10^{-3} to 2×10^{-2} M for each H^+ concentration which was over the range 0.05–0.6 M. In every case, first-order kinetics was observed. The reported rate constants are the average of 8 replicate determinations.

The acid hydrolysis kinetics of ferric O-TRENSEX complex was studied under pseudo-first-order conditions in the presence of excess protons ($[\text{H}^+]$ range 0.02–1 M) at 25 °C. The initial pH of the ferric O-TRENSEX solution was 4.0.

Results

Ligand Deprotonation Constants. The sulfonated ligands O-Trensox and N-Trensox possess seven protonation sites (three pyridine nitrogen atoms, one tertiary amine nitrogen atom, and three hydroxyl oxygen atoms) and are denoted LH_7^+ , taking into account the negative charges of the three sulfonate groups. The deprotonation constants of O-Trensox were determined by two potentiometric titrations, over the pH range 2–7 (for the lower $\text{p}K_a$ values) and over the pH range 3–10 (Figure 1b). The deprotonation constants for N-Trensox were determined by potentiometric titrations (Figure 1a). Spectrophotometric titration was also carried out showing a buffer region from pH 5 to 8. The corresponding spectra (not shown) exhibited isobestic behavior at $\lambda = 265 \text{ nm}$ ($\lambda_{\text{max}} = 254 \text{ nm}$ at pH 5 and $\lambda_{\text{max}} = 278 \text{ nm}$ at pH 8).³⁰ The data were analyzed over the pH range 5–8 by the method of Schwarzenbach³¹ yielding a $\text{p}K_a$ value of 6.46. The $\text{p}K_a$ values of O-Trensox and N-Trensox are tabulated in Table 1.

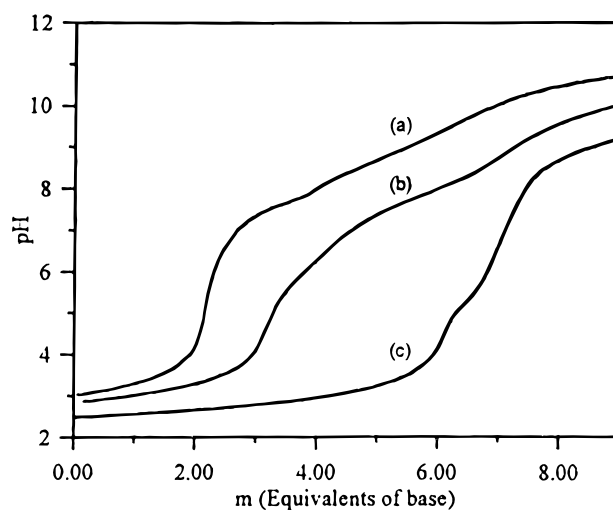


Figure 1. Potentiometric titration curves for (a) 1 mM N-TRENSEX, (b) 1 mM O-TRENSEX, (c) O-TRENSEX + Fe^{3+} , 1:1, 0.8 mM. All solutions were at 25 °C and $I = 0.1 \text{ M}$ (NaClO_4). A slight precipitate was observed below pH 6 during the titration of N-TRENSEX. The $\text{p}K$'s of the ligands were calculated using the program SUPERQUAD²⁷ with $\sigma_{\text{fit}} < 2.5$.

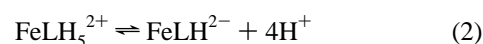
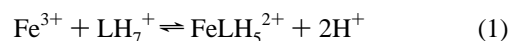
Table 1. Deprotonation Constants^a of O-TRENSEX and N-TRENSEX

	O-TRENSEX	N-TRENSEX	O-TRENSEX	N-TRENSEX
$\text{p}K_1$	8.62 ± 0.04	9.69 ± 0.01	$\text{p}K_5$	3.01 ± 0.04
$\text{p}K_2$	8.18 ± 0.05	8.73 ± 0.01	$\text{p}K_6$	2.55 ± 0.08
$\text{p}K_3$	7.44 ± 0.04	8.26 ± 0.02	$\text{p}K_7$	1.83 ± 0.10
$\text{p}K_4$	6.36 ± 0.03	6.99 ± 0.02		3.10 ± 0.06^c

^a $\text{LH}_n \rightleftharpoons \text{LH}_{n-1} + \text{H}^+$, $K_n = [\text{LH}_{n-1}][\text{H}^+]/[\text{LH}_n]$. ^b $\text{p}K_5 = 6.46$ from spectrophotometric titration. ^c These values are less reliable since a slight precipitate was observed below pH 6.

Ferric Complexes' Equilibria. A combined use of spectrophotometric and potentiometric titration allowed us to determine the O-TRENSEX ferric species and their formation constants.

A first set of UV–visible spectra were recorded for solutions containing a constant concentration of ligand and varying amounts of Fe(III) ($\text{Fe}:\text{O-TRENSEX}$ ratio was varied from 1:1 to 10:1) and H^+ (HClO_4 , 0.3–1.5 M). The spectra exhibited a charge transfer band at 435 nm (orange complex; see spectrum 1 in Figure 2), and the absorbance increased (i) as the proton concentration decreased at constant $[\text{Fe}^{3+}]$ and (ii) as the Fe(III) concentration increased at constant $[\text{H}^+]$. The equilibrium constant could thus be determined, since the complexation was incomplete at equilibrium. A second set of spectra were generated for 1:1 solutions of ferric ion and ligand from pH 1 to 10. As the pH was increased from 1 to 2, the charge transfer bands were found to shift to 443 nm ($\epsilon = 5200 \text{ M}^{-1}\text{cm}^{-1}$) and 595 nm ($\epsilon = 5200 \text{ M}^{-1}\text{cm}^{-1}$) (green complex) forming two isobestic points at 370 and 534 nm (Figure 2). The absorbance data for the two sets of spectra were processed with the Letagrop program.²⁸ The best fit was obtained by considering the equilibria of the formation of the $[\text{FeLH}_5]^{2+}$ species (orange complex) at $\text{pH} < 1$ and of the $[\text{FeLH}]^{2-}$ species (green complex) at $\text{pH} > 1$:



In addition, the spectra were analyzed over the pH range 1–2

(29) Kidric, J.; Hadzi, D.; Hocjan, D.; Rutar, V. *Org. Magn. Reson.* **1981**, *15*, 280–284.

(30) Boukhalfa, H. Thesis, Université Joseph Fourier, Grenoble, 1996.

(31) Schwarzenbach, G.; Schwarzenbach, K. *Helv. Chim. Acta* **1963**, *46*, 1390–1400.

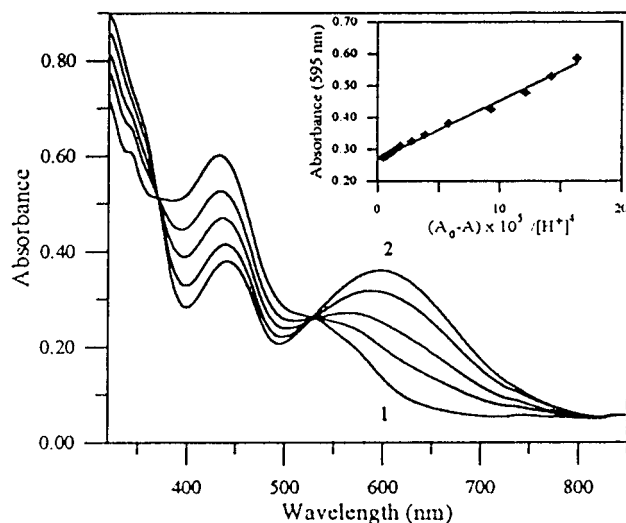


Figure 2. UV-visible spectra of a 1:1 solution of ferric ion and O-TRENDOX as a function of pH (from 1 to 2): 1.01, 1.28, 1.49, 1.61, 2.11. $[O-TRENDOX] = [Fe^{3+}]_{tot} = 0.07$ mM; $I = 0.1$ M ($NaClO_4 + HClO_4$); 25 °C. (Inset: Schwarzenbach plot within the pH range 1.0–2.0, where A is the absorbance at 595 nm at each pH value and A_0 the final absorbance of $FeLH^{2-}$ measured at pH 3.)

Table 2. Equilibrium Constants, $\log \beta_{11n}^a$ and UV-Visible Spectral Characteristics of Complexes

ligand	complex	$\log \beta_{11n}^a$	pFe^b	λ (nm)	ϵ ($M^{-1} cm^{-1}$)
O-TRENDOX	$FeLH_5^{2+}$	42.2 ± 0.1		435	8200
	$FeLH^{2-}$	36.5 ± 0.1		443	5200
				595	5200
	FeL^{3-}	30.9 ± 0.1	29.5	443	5400
			595	5400	
N-TRENDOX	FeL^{3-}	25.3 ± 0.1	22.2	595	1200

^a $\beta_{11n} = [FeLH_n]/[Fe^{3+}][L][H^+]^n$ is the equilibrium constant for $Fe^{3+} + L + nH^+ \rightleftharpoons FeLH_n$. ^b $pFe = -\log [Fe^{3+}]$, calculated for $[Fe^{3+}] = 10^{-3}$ mM, $[L] = 10^{-2}$ mM, and pH = 7.4.

by the method of Schwarzenbach^{31,32} (Figure 2). The results confirm the $FeLH_5^{2+}/FeLH^{2-}$ equilibrium constant determined with Letagrop program. The values of β_{115} and β_{111} defined as

$$\beta_{11n} = \frac{[FeLH_n]}{[Fe^{3+}][L][H^+]^n} \quad (3)$$

are reported in Table 2. It must be noted that the value of β_{115} is less accurate than that of β_{111} , due to the variation of the ionic strength over the $[H^+]$ range 0.3–1.5 M. A tiny spectral change was observed over the pH range 2–9 and was not suitable for analysis.

The potentiometric titration was carried out for 1:1 solutions in ferric ion and ligand from pH 2 to 10. The curve (Figure 1c) showed an inflection at $m = 6$ and $m = 7$ (m is the number of moles of base per mole of metal). This indicates the formation of successively two species in which 6 and 7 protons have been displaced from O-TRENDOX by the ferric ion, i.e. the $FeLH^{2-}$ and the FeL^{3-} species, respectively. The potentiometric titration thus confirms the formation of the $FeLH^{2-}$ species in agreement with the spectrophotometric titration. Since the complex $FeLH^{2-}$ is fully formed at pH 2, only the $FeLH^{2-}/$

(32) The Schwarzenbach plot was used to determine the number of protons involved in equilibrium 2 according to the relation $A = (A_0 - A)/(K_2[H^+]^n) + A_f$, where A_0 is the initial absorbance of the $FeLH^{2-}$ complex, A_f the final absorbance of the $FeLH_5^{2+}$ complex, and A the observed absorbance at any $[H^+]$. The absorbances were measured at 595 nm. A linear plot was obtained only for $n = 4$.

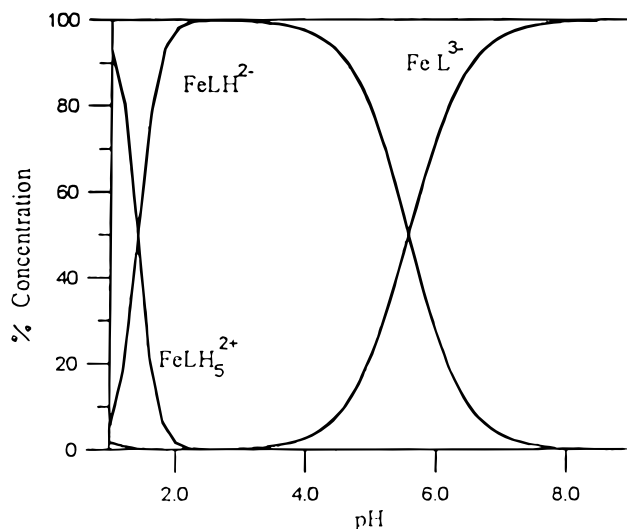
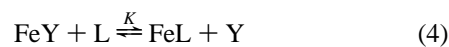


Figure 3. Species distribution curves for the ferric O-TRENDOX complex ($[O-TRENDOX-Fe] = 0.1$ mM).

FeL^{3-} equilibrium constant was determined from titration data. The formation constant $\log \beta_{110}$ was calculated to be 30.9.

The stability constant of the ferric complexes could also be determined by spectrophotometric competition experiments against EDTA over the pH range 2–3. The following equations correspond to the competition equilibrium (charges omitted for clarity):



$$K = \frac{[FeL][Y]}{[FeY][L]} = \frac{\beta_{110}^{FeL}}{\beta_{110}^{FeY}} \quad (5)$$

FeL represents the O-TRENDOX complex, and Y , the tetraanion of EDTA. The concentration of FeL was calculated from the absorbance at 595 nm, where FeL is the only absorbing species. The concentrations of the other species in eq 5 were calculated from mass balance equations and pH:

$$[Fe]_{tot} = \alpha_{FeL}[FeL] + \alpha_{FeY}[FeY] \quad (6)$$

$$[L]_{tot} = \alpha_{FeL}[FeL] + \alpha_L[L] \quad (7)$$

$$[Y]_{tot} = \alpha_{FeY}[FeY] + \alpha_Y[Y] \quad (8)$$

Here α 's are the usual Ringbom's coefficients.³³ Using the known formation constants of Fe^{III} -EDTA (β_{110} and β_{111})³⁴ and the protonation constant K_{FeLH} , $\log \beta_{110}$ of the ferric O-TRENDOX was determined to be 30.8. This is in excellent agreement with the value determined from spectrophotometric and potentiometric titration. The distribution curves are shown in Figure 3.

A quite different behavior was observed for ferric N-TRENDOX solutions. The formation of a green complex was obtained only upon addition of successive small amounts of a $Fe(III)$ solution to a solution of ligand at pH about 7–8. The complex was found to be stable in a narrow range of pH, approximately 6–9. The complex Fe -N-TRENDOX yields a charge transfer band at 600 nm ($\epsilon = 1200 M^{-1} cm^{-1}$). The stability constant β_{110} could however be determined from

(33) Ringbom A. *Complexation in Analytical Chemistry*; Interscience: New York, 1963.

(34) Martell, A. E.; Smith, R. M. *Critical Stability Constants*; Plenum Press: New York, 1974.

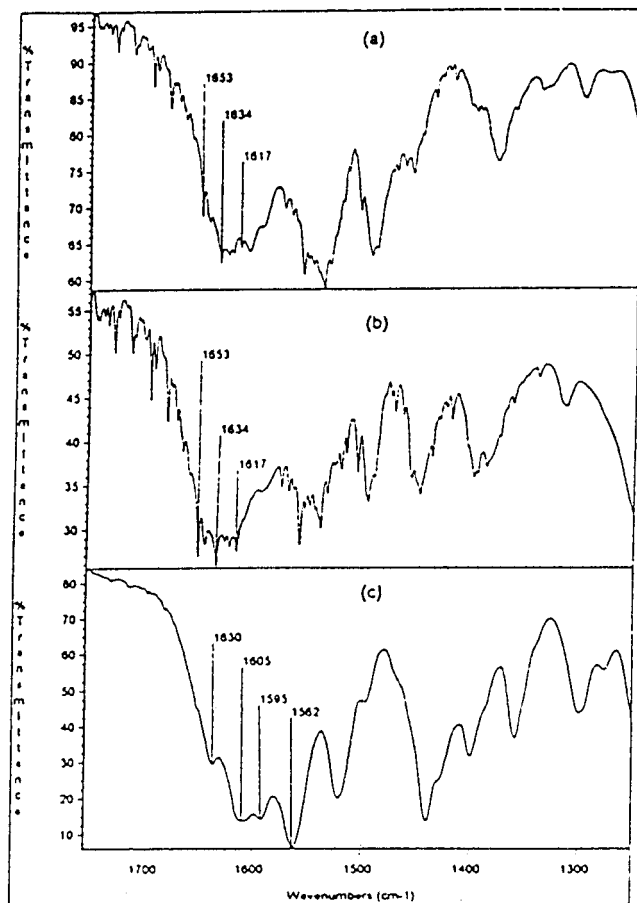


Figure 4. Infrared spectra of KBr pellets of O-TRENSEX, as H_3L (a), FeL^{3-} (b), and FeLH_5^{2+} (c).

spectrophotometric competition against EDTA over the pH range 7–8. The value of $\log \beta_{110}$ was calculated to be 25.3, assuming that the ferric N-TRENSEX complex is of the FeL type. A complete study of the complexation of Fe(III) by N-TRENSEX was not undertaken.

Spectrometry. Solid samples of the orange FeLH_5^{2+} and green FeL^{3-} ferric O-TRENSEX complexes could be extracted from a saturated aqueous solution. Unfortunately, no crystals suitable for crystallographic analysis could be obtained. Infrared spectra were recorded on the dried solids as KBr pellets in order to gain more information on the mode of coordination in the orange and the green ferric O-TRENSEX complexes. The IR spectra of O-TRENSEX (H_3L form), the orange FeLH_5^{2+} complex, and the green FeL^{3-} complex are shown in Figure 4. Interest was focused on the bands over the range 1650–1600 cm^{-1} which have been assigned to the $\nu_{\text{C}=\text{O}}$ amide stretch. The spectra of H_3L and FeL^{3-} (Figure 4a,b) both exhibit the $\nu_{\text{C}=\text{O}}$ band in the region 1650–1610 cm^{-1} , indicating a similar environment of the amide carbonyl group in the free and coordinated ligand. A significant difference appears between these spectra and the spectrum of FeLH_5^{2+} (Figure 4c). The $\nu_{\text{C}=\text{O}}$ absorption is shifted to 1630–1595 cm^{-1} . This indicates a change in the environment of the carbonyl group in the FeLH_5^{2+} and in the FeL^{3-} species. In addition, the absorption at 1360 cm^{-1} in the FeLH_5^{2+} spectrum, which could be assigned to OH deformation, disappears in the FeLH_5^{2-} spectrum.

For the ^1H NMR spectra, Fe(III) was replaced with Ga(III) in the O-TRENSEX complexes, Ga(III) being diamagnetic and structurally and chemically close to Fe(III) . $^2\text{H}_2\text{O}$ solutions of Ga(III) and of the ligand in the 1:1 molar ratio were examined over the pH range 2–10. Since the equilibrium constants for

the complexes formation are very large, the spectra exhibited signals of coordinated protons only. The ^1H spectra of the solutions at pH 2.0, 3.0, and 5.0 are shown in Figure 5. Increasing the pH from 2.0 to 5.0 induced large shifts of the coordinated ligand signals, indicating a change in the complex species. At pH 2 (Figure 5a), three different sets of signals were observed for the aromatic (noted n, n', and n'') and methylene protons. The signals occur in a 1:1 integration ratio, and the connectivities between the protons in each sulfoxine moiety were deduced from COSY 2D experiments (except for the H-6 proton). It should be noted that sharp signals were observed for two protons H-6. The shoulder at 8.40 ppm (Figure 5a) and the broadened signal at 8.35 (Figure 5b) were assigned to the third proton H-6. The ^{13}C spectrum (not shown) exhibited the same features as the ^1H spectrum i.e. three sets of signals. It could be concluded that the three arms of the ligands are nonequivalent. On increase of the pH, the intensity of the signals decreased and vanished at approximately pH 5, whereas another set of signals (noted a) appeared above pH 3 (Figure 5b,c). The spectra recorded over the pH range 5–10 remained unchanged and exhibited only one set of signals which may be assigned to the GaL^{3-} complex, on the basis of the study of the $\text{Fe}^{\text{III}}-\text{O-TRENSEX}$ complexation and assuming similar behavior for Ga^{III} and Fe^{III} . This indicates that the pendant arms of the coordinated ligand are equivalent. These results are consistent with the IR study. The spectrum at pH 2 could thus be attributed to a protonated species assumed to be GaLH_5^{2+} .

Another significant change between the ^1H NMR spectra of the complexes and the free ligand is observed in the methylene protons signals. In the free ligand, the two protons of each methylene group are magnetically equivalent as a result of free rotation. In the diamagnetic complexes of Ga(III) , however, the chelation causes these protons to become nonequivalent. Four resonances were observed for the GaL^{3-} complex at 3.96, 3.17, 2.78, and 2.43 ppm. For the GaLH_5^{2+} complex the methylene resonances were displayed over the range 4.3–2.4 ppm.

Electrochemistry. Cyclic voltammograms were recorded in aqueous solution at scan rate between 10 and 200 mV/s (Figure 6). The same voltammetric data were obtained by starting from either Fe(III)-O-TRENSEX or Fe(II)-O-TRENSEX solutions. The results show a quasi reversible one electron transfer which is attributed to the $\text{Fe}^{\text{III}}-\text{O-TRENSEX}/\text{Fe}^{\text{II}}-\text{O-TRENSEX}$ process ($\Delta E_p = 75, 85, 90, 95,$ and 105 at scan rates of 10, 20, 50, 100, and 200 mV/s, respectively). The one electron transfer has been confirmed by potentiostatic and coulometric measurements starting either from a Fe(III)-O-TRENSEX or a Fe(II)-O-TRENSEX solution. A value of the redox potential, denoted E_c° , of 0.087 ± 0.005 V/NHE or 0.084 ± 0.005 V/NHE has been calculated for measurements using an Ag/AgCl , KCl saturated reference electrode or Ag/AgCl , NaCl saturated reference electrode, respectively. This value is independent of the pH over the range 4–10. Taking into account the E_c° values for the redox couples $\text{Fe}^{\text{III}}\text{L}/\text{Fe}^{\text{II}}\text{L}$ ($E_c^\circ = 0.087$ V) and $\text{Fe}^{\text{III}}/\text{Fe}^{\text{II}}$ ($E_c^\circ = 0.77$ V), the ratio $\beta_{110}(\text{Fe}^{\text{II}}\text{L})$ can be calculated from

$$E_c^\circ = E_c^\circ + 0.059 \log[\beta_{110}(\text{Fe}^{\text{II}}\text{L})/\beta_{110}(\text{Fe}^{\text{III}}\text{L})] \quad (9)$$

and gives $\log \beta_{110}(\text{Fe}^{\text{II}}\text{L}) = 19.3$.

Kinetic Studies. Formation Kinetics. The kinetics of Fe(III)-O-TRENSEX complex formation was investigated by a stopped-flow spectrophotometric method under pseudo-first-order conditions $[\text{Fe(III)}] \gg [\text{O-TRENSEX}]$ at the wavelength 435 nm and $I = 2$ M ($\text{NaClO}_4, \text{HClO}_4$). The absorbance change with time showed a single exponential curve indicating that the complex formation reaction proceeds through a single rate-

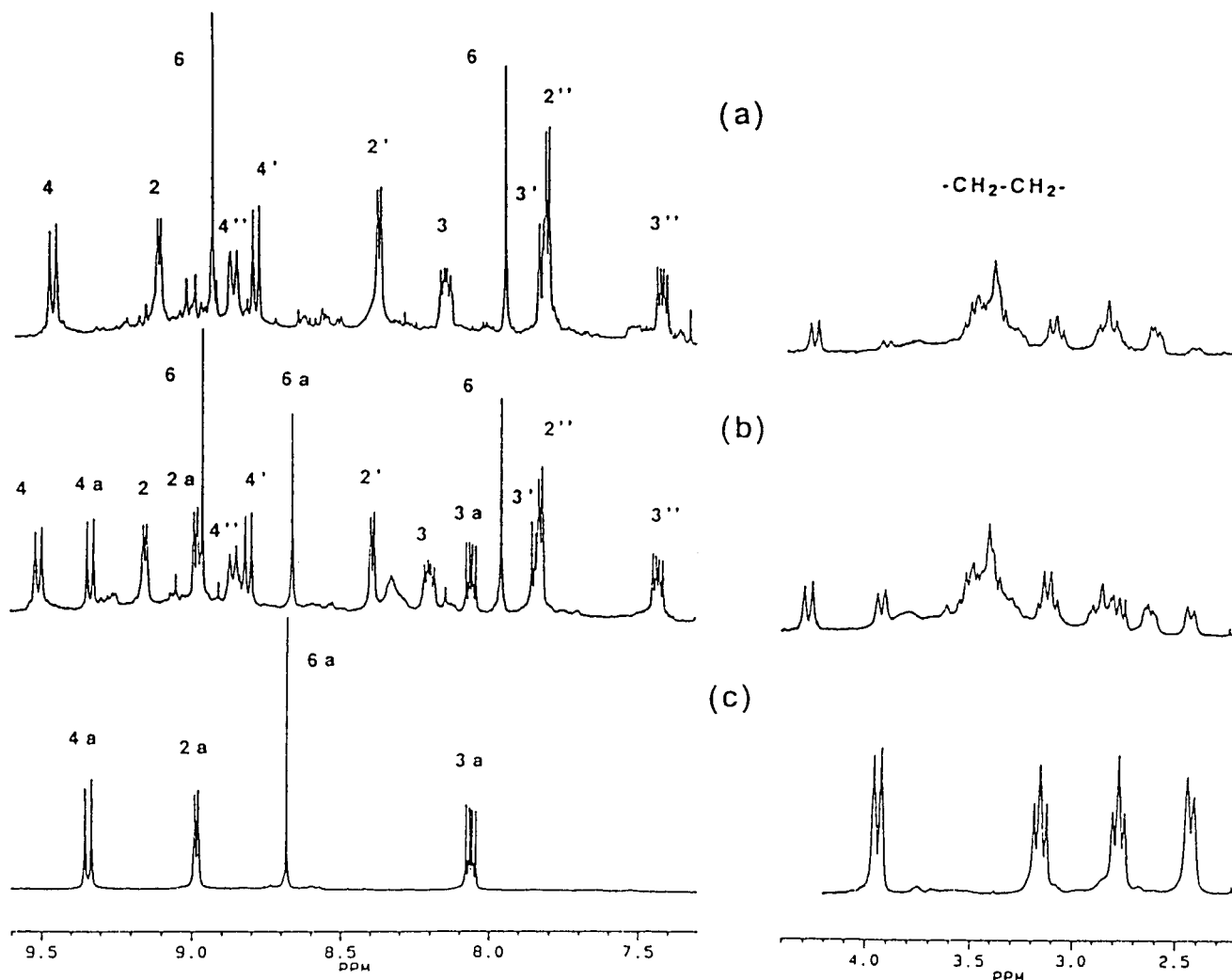
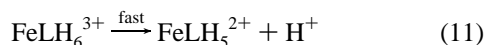


Figure 5. ^1H NMR spectra (400 MHz) of O-TRENSEX (0.01 M) and Ga^{3+} (0.01 M) in $^2\text{H}_2\text{O}$ solutions at pH 2 (a), 3 (b) and 5 (c), showing quinoline ring and methylene protons. For numbering, see the drawing of O-TRENSEX.

limiting stage. The corresponding pseudo-first-order constants k_{obs} (s^{-1}) determined at $[\text{H}^+]$ over the range 0.05–0.6 M and various concentrations of Fe(III) are plotted in Figure 7. Slopes and intercept variations with $[\text{H}^+]$ suggest that the main reaction mechanism is the complex formation through the hydrolyzed ferric ion FeOH^{2+} and the LH_7^+ ligand species:



The predicted rate law is then given by

$$k_{\text{obs}} = k_1 K_{\text{Fe}} \frac{[\text{Fe}^{3+}]}{[\text{H}^+]} + k_{-1} \quad (12)$$

$$K_{\text{Fe}} = \frac{[\text{FeOH}^{2+}][\text{H}^+]}{[\text{Fe}^{3+}]} \quad [\text{Fe}^{3+}] = [\text{Fe}^{3+}]_{\text{tot}} - [\text{FeOH}^{2+}]$$

The value of K_{Fe} in 2.0 M NaClO_4 is $1.51 \cdot 10^{-3}$ M.³⁵ Fe^{3+} and FeOH^{2+} represent $[\text{Fe}(\text{H}_2\text{O})_6]^{3+}$ and $[\text{Fe}(\text{H}_2\text{O})_5\text{OH}]^{2+}$, respectively (omitting solvating water).

The least-squares fit of k_{obs} versus $[\text{Fe}^{3+}]/[\text{H}^+]$ (Figure 8) yields the values

$$k_1 = 789 \pm 17 \text{ M}^{-1} \text{ s}^{-1} \quad k_{-1} \approx 0$$

Acid Hydrolysis Kinetics. The acid hydrolysis kinetics of the ferric O-TRENSEX complex was studied in water ($I = 2.0$ M, 25°C) by the pH jump method. The k_{obs} rate constants were determined from the absorbance data versus time at either 595 nm or 443 nm. The absorption spectra were also monitored (λ range 300–700 nm) using a diode array stopped-flow spectrophotometer. The pH jump reactions were performed under pseudo-first-order conditions with respect to H^+ for solutions containing Fe(III) and O-TRENSEX in a 1:1 molar ratio at pH 4.0. According to the distribution curves, the FeLH_5^{2+} complex predominates. It should be pointed out that experiments carried out for solutions at pH 7.0 (FeL^{3-} species) provided the same results as those at pH 4.0, indicating that the first protonation of the FeL^{3-} complex is a very fast process. This protonation has been assumed to occur at the tertiary amine nitrogen atom (*vide infra*).

Upon addition of acid to dilute solutions of FeLH_5^{2+} complex, the green color was changed to orange, as expected. However, the affinity of O-TRENSEX for Fe(III) is such that complete dissociation of the ferric complex did not occur even in 3 M HClO_4 . The spectrophotometric signal recorded vs time at 595 nm exhibited four successive decays. A loss of amplitude (30%

(35) Milburn, R. M.; Vosburgh, W. C. *J. Am. Chem. Soc.* **1955**, *77*, 1352–1355.

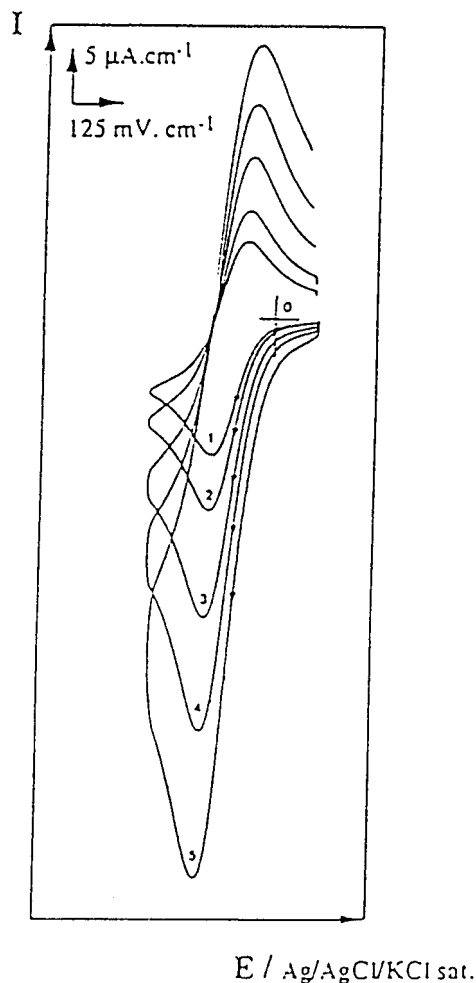


Figure 6. Cyclic voltammetry of ferric O-TRENTOX in aqueous solution (1 mM) with 0.1 M NaClO₄: $v = 10$ (1), 20 (2), 50 (3), 100 (4), and 200 mV/s (5).

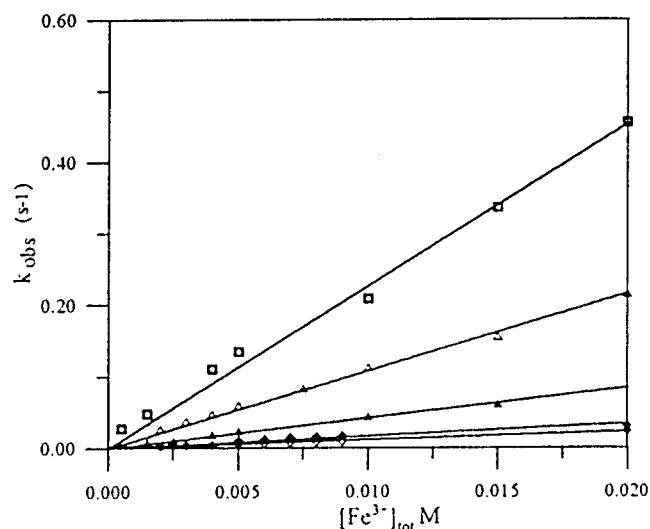


Figure 7. Variation of the experimental rate constant k_{obs} (s^{-1}) as a function of $[\text{Fe}^{3+}]_{\text{tot}}$ at various $[\text{H}^+]$ (M): (□) 0.05, (△) 0.1, (▲) 0.2, (◆) 0.5, (◇) 0.6. [O-TRENTOX] = 0.05 mM. Solvent: water ($I = 2.0$ M, $T = 25$ °C).

of the initial absorbance amplitude for all of the spectrum) was observed during the first milliseconds, but the process (denoted stage 1) was too fast to be monitored by stopped-flow measurements. Then, a first-order absorbance decay was measured in the time range of deciseconds (denoted stage 2) and a two-exponential absorbance decay was detected in the time range

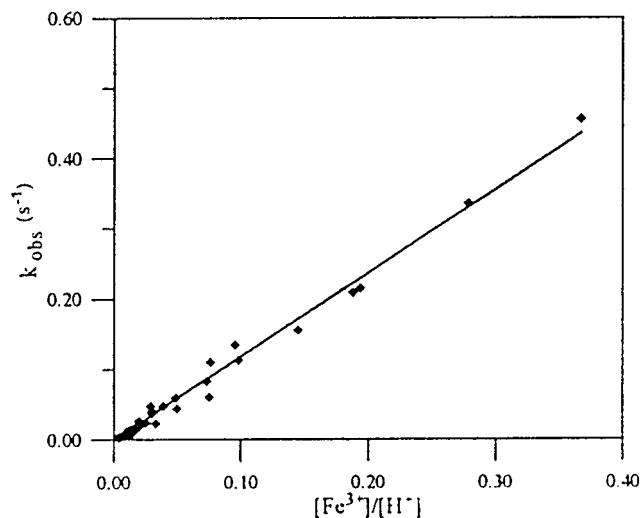


Figure 8. k_{obs} ($\text{M}^{-1} \text{s}^{-1}$) as a function of $[\text{Fe}^{3+}]/[\text{H}^+]$ according to eq 12 for the complexation of Fe(III) by O-TRENTOX.

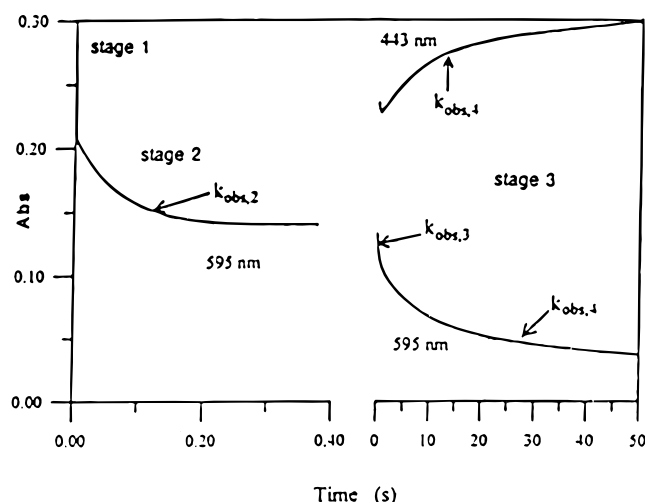


Figure 9. Acid hydrolysis kinetics of the ferric O-TRENTOX complex (FeLH^{2-} species). $[\text{FeLH}^{2-}] = 0.05$ mM; $[\text{H}^+] = 0.06$ M for stages 1 and 2, $[\text{H}^+] = 0.2$ M for stage 3. Solvent: water ($I = 2.0$ M, $T = 25$ °C).

of seconds (denoted stage 3) (Figure 9). Furthermore, the absorbance recorded versus time at 443 nm for the stage 3 (Figure 9) exhibited a very small decay over the 0.2 s time scale (corresponding to the fast decay recorded at 595 nm), followed by a first-order absorbance increase over the 0.2–20 s time scale. The rate constants of the stage 2 (denoted $k_{\text{obs},2}$) were determined from the absorbance decay at 595 nm over the $[\text{H}^+]$ range 0.02–0.2 M. The rate constants $k_{\text{obs},3}$ and $k_{\text{obs},4}$ related to stage 3 were determined over the $[\text{H}^+]$ range 0.1–1 M by fitting the two-exponential decay at 595 nm. In addition, the values of $k_{\text{obs},4}$ were also calculated from the first-order absorbance increase at 443 nm. These values were found to be in reasonable agreement with the values determined at 595 nm. However, these late values are less reliable since they are obtained by fitting a two-exponential signal having a small amplitude decay. So, owing to their higher accuracy, the data at 443 nm were used for the study of $[\text{H}^+]$ dependence.

The UV–visible spectra were recorded as a function of the time for selected $[\text{H}^+]$ in order to monitor the change of the spectrum in each stage of the hydrolysis reaction and to provide additional information on the intermediate species (Figure 10). This change suggests the formation of four intermediate protonated ferric O-TRENTOX complexes. The spectrum

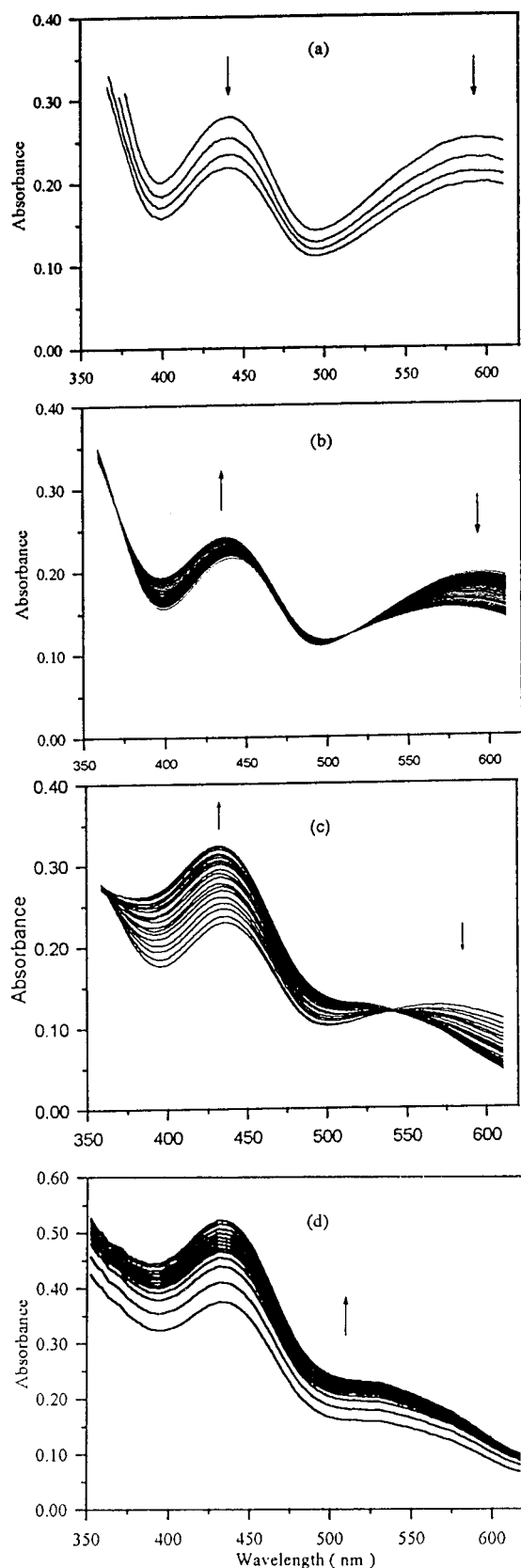


Figure 10. UV-visible spectra recorded as a function of the time for the acid hydrolysis kinetics of the FeLH^{2-} complex ($\text{Fe}^{\text{III}}\text{-O-TREN-SOX}$): (a) stage 1, 6–10 ms (1.3 ms interval); (b) stage 2, 10–200 ms (5 ms interval); (c) stage 3, 1–20 s (1 s interval); (d) stage 4, 20–200 s (10 s interval). Experimental conditions: See Figure 9 except for stage 4, where $[\text{H}^+] = 0.5 \text{ M}$ and $[\text{FeLH}^{2-}] = 0.065 \text{ mM}$. The arrows show the direction of change as the reaction proceeds.

recorded at the end of the stage 1 (Figure 10a) is the same as that of the initial complex but with lower absorption coefficient

for all of the wavelengths. The formation of the second intermediate (stage 2) results in a decrease of the absorbance at 595 nm and a slight increase at 443 nm (Figure 10b). The spectra collected during this process exhibit a sharp isosbestic point at 520 nm, confirming the presence of only two absorbing species. The third stage leads to a species the spectrum of which resembles that of FeLH_5^{2+} but with a lower absorption coefficient at 443 nm (Figure 10c). An isosbestic point at 540 nm was observed for the spectra recorded over the second step of this stage. Finally, after a reaction time longer than 50 s an increase of the absorbance was observed (Figure 10d) exhibiting a behavior unsuitable for kinetic analysis.

The proton stoichiometry of steps 1 and 2 was determined by analyzing the absorbance values measured at the end of the two first steps $A_{\infty,2}$ vs $[\text{H}^+]$ and by taking into account following the two equilibria:



The absorbance at equilibrium for step 2 is expressed by

$$\frac{A_{\infty,2}}{[\text{FeLH}^{2-}]_{\text{tot}}} = \frac{\epsilon_{\text{FeLH}} + \epsilon_1 K_1 [\text{H}^+]^n + \epsilon_2 K_1 K_2 [\text{H}^+]^{n+n'}}{1 + K_1 [\text{H}^+]^n + K_1 K_2 [\text{H}^+]^{n+n'}} \quad (15)$$

Analysis of $A_{\infty,2}$ vs $[\text{H}^+]$ using a nonlinear least-squares method leads to $n = 2$ and $n' = 1$. The absorption coefficients ϵ_1 and ϵ_2 at 595 nm of the species FeLH_{1+n}^{n-2} i.e. FeLH_3 , and $\text{FeLH}_{1+n+n'}^{n+n'-2}$, i.e. FeLH_4^+ , respectively, and the stability constants K_1 and K_2 were calculated:

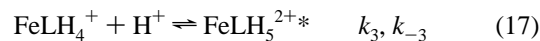
$$K_1 = 18000 \pm 6000 \text{ M} \quad \epsilon_1 = 3200 \pm 600 \text{ M}^{-1} \text{ cm}^{-1}$$

$$K_2 = 42 \pm 37 \text{ M} \quad \epsilon_2 = 2000 \pm 150 \text{ M}^{-1} \text{ cm}^{-1}$$

The values of the pseudo-first-order rate constants $k_{\text{obs},2}$ and $k_{\text{obs},3}$, $k_{\text{obs},4}$ related to stages 2 and 3, respectively, are reported in Table 3. $k_{\text{obs},2}$ exhibits a linear dependence on $[\text{H}^+]$ (Figure 11), and the intercept is slightly negative, suggesting that reaction 14 is first-order in proton in agreement with $n' = 1$ and is irreversible. Linear least-squares regression of the data against eq 16 gives $k_2 = 643 \pm 22 \text{ M}^{-1} \text{ s}^{-1}$.

$$k_{\text{obs},2} = k_2 [\text{H}^+] \quad (16)$$

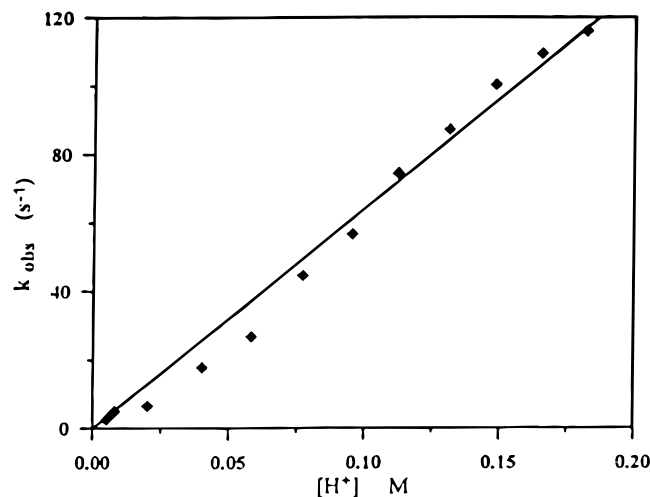
A linear dependence on $[\text{H}^+]$ is exhibited by $k_{\text{obs},3}$ (Figure 12a) suggesting a reaction first-order in proton consistent with the reaction 17. $k_{\text{obs},4}$ exhibits saturation-like kinetics (Figure 12b) with respect to $[\text{H}^+]$. This is consistent with a proton-dependent equilibrium followed by a proton-independent reaction with a reaction rate slower than the reaction rates involved in the equilibrium. According to these results, we propose for stage 3 the two reactions 17 and 18:



Here FeLH_5^{2+*} and FeLH_5^{2+**} are species different from the thermodynamic product FeLH_5^{2+} . The associated first-order rate constants $k_{\text{obs},3}$ and $k_{\text{obs},4}$ are related to the microscopic rate

Table 3. Pseudo-First-Order Rate Constants for the Acid Dissociation of Ferric O-TRENISOX^a

[H ⁺] (M)	<i>k</i> _{obs,2} ^b (s ⁻¹)	<i>k</i> _{obs,3} ^b (s ⁻¹)	<i>k</i> _{obs,4} ^b (s ⁻¹)	<i>k</i> _{obs,4} ^c (s ⁻¹)
0.005	2.55 ± 0.07			
0.007	4.26 ± 0.06			
0.008	5.0 ± 0.1			
0.020	6.5 ± 0.2			
0.040	17.8 ± 0.6			0.0370 ± 0.0005
0.050				0.0410 ± 0.0005
0.058	26.9 ± 0.5			
0.077	44.7 ± 0.7			
0.095	57 ± 1			
0.100				0.0587 ± 0.0007
0.112	74 ± 2			
0.131	87 ± 2			
0.148	100 ± 2			
0.150		2.23 ± 0.05	0.110 ± 0.007	0.080 ± 0.004
0.165	109 ± 2			
0.182	116 ± 3			
0.200				0.094 ± 0.006
0.250		2.88 ± 0.05	0.15 ± 0.01	0.105 ± 0.003
0.300		3.13 ± 0.05	0.15 ± 0.01	0.121 ± 0.008
0.350		3.50 ± 0.05	0.16 ± 0.01	0.119 ± 0.008
0.400		4.00 ± 0.04	0.17 ± 0.01	0.133 ± 0.004
0.450				0.147 ± 0.004
0.500				0.151 ± 0.005
0.600				0.163 ± 0.003
0.700				0.173 ± 0.018
0.800				0.184 ± 0.002
0.900				0.195 ± 0.017
1.000		7.0 ± 0.5	0.24 ± 0.01	0.199 ± 0.018

^a [Ferric O-TRENISOX] = 5 × 10⁻⁵ M; T = 25 °C, and I = 2.0 M.^b Determined at λ = 595 nm. ^c Determined at λ = 443 nm.**Figure 11.** Kinetic data for stage 2 in the acid hydrolysis of the ferric O-TRENISOX complex (FeLH²⁺ species). [FeLH²⁺] = 0.05 mM; I = 2 M; T = 25 °C. *k*_{obs,2} = f[H⁺] according to eq 16.

constants of chemical reactions 17 and 18 by the following relationships:

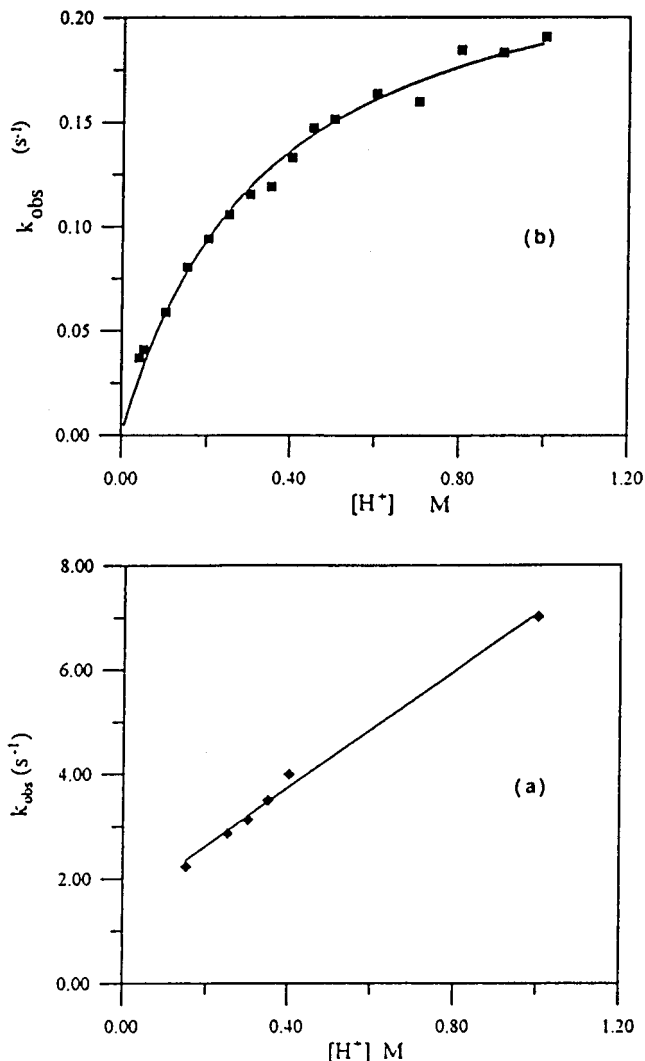
$$k_{\text{obs},3} + k_{\text{obs},4} = k_3 [\text{H}^+] + k_{-3} + k_4 + k_{-4} \quad (19)$$

$$k_{\text{obs},3}k_{\text{obs},4} = k_3(k_4 + k_{-4}) [\text{H}^+] + k_{-3}k_{-4} \quad (20)$$

Linear plots of (*k*_{obs,3} + *k*_{obs,4}) vs [H⁺] and (*k*_{obs,3}*k*_{obs,4}) vs [H⁺] were obtained. The four microscopic rate constants could be extracted from the slopes and intercepts of the two plots:

$$k_3 = 5.7 \pm 0.4 \text{ M}^{-1} \text{ s}^{-1} \quad k_{-3} = 1.34 \pm 0.1 \text{ s}^{-1}$$

$$k_4 = 0.26 \pm 0.01 \text{ s}^{-1} \quad k_{-4} \approx 0$$

**Figure 12.** Kinetic data for stage 3 in the acid hydrolysis of the ferric O-TRENISOX complex (FeLH²⁺ species). [FeLH²⁺] = 0.05 mM; I = 2 M; T = 25 °C. Key: (a) *k*_{obs,3} = f[H⁺]; (b) *k*_{obs,4} = f[H⁺].

Discussion

Ligand Deprotonation Constants. The three lower *pK*_a values and the three higher *pK*_a values of O-TRENISOX were assigned to pyridine nitrogen and hydroxyl groups, respectively, by comparison with the *pK*_a values of the 8-hydroxyquinoline-5-sulfonate. The *pK*_a of 6.36 was attributed to the tertiary amine from ¹H NMR measurements since the nitrogen deprotonation results in large chemical shifts effect on the methylenes of the "TREN" backbone.¹⁷ The *pK*_a values of the pyridine protonated nitrogen atoms (1.83, 2.55, and 3.01) and of the hydroxyl groups (7.44, 8.18, and 8.62) cover a range 0.44–0.74 that reflects a roughly statistical separation (log 3 or 0.48),³⁶ which is consistent with noninteracting pendant arms. The *pK*_a values for the pyridine nitrogen atoms are significantly lower than the value 3.95 in the 8-hydroxyquinoline-5-sulfonate presumably related to the electron-withdrawing effect of the amide group ortho to the hydroxyl group. The average value of the hydroxyl *pK*_a's, 8.07, is lower than the corresponding *pK*_a of 8.42 in 8-hydroxyquinoline-5-sulfonate³⁷ in relation to the electron-withdrawing amide group. However, this effect appears to be smaller (0.35 log unit) for O-TRENISOX than for catechol⁹ or biphenol derivatives¹⁷ (0.8). The basicity of the tertiary amine

(36) Adams, E. Q. *J. Am. Chem. Soc.* **1916**, 38, 1503–1510.(37) Letkeman, P.; Martell, A. E.; Motekaitis, R. J. *J. Coord. Chem.* **1980**, 10, 47–53.

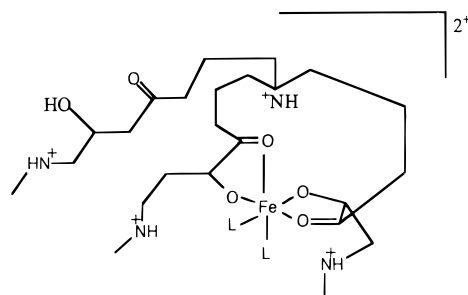
is strongly lowered as expected for tripodal ligands with a "TREN" backbone.^{9,14} This is related to the formation of hydrogen bonding between the amine and the N-H amide proton.

Concerning the ligand N-TRENSEX, the two lower pK_a values and the three higher pK_a values have been clearly assigned to the pyridine protonated nitrogen and to the hydroxyl groups. The hydroxyl pK_a values are higher than those of O-TRENSEX as a result of the effect of the amide group. The values of 6.44 and 6.99 can be attributed to either one pyridine nitrogen or the tertiary amine. NMR measurements did not allow us to determine the pK_a of the tertiary amine since N-TRENSEX was not soluble enough in 2H_2O solutions, but UV-visible measurements suggested that the pK_a of the protonated pyridine atoms is 6.44 as the pyridine nitrogen deprotonation is expected to give an absorbance effect contrary to that for the tertiary amine deprotonation. The pK_a value for one pyridine nitrogen is much higher than the two other ones. A possible explanation could be the formation of a network of two hydrogen bonds between the carbonyl oxygen and both the pyridinium and the tertiary ammonium protons, giving rise to a five-membered ring and a seven-membered ring which stabilize the protonated pyridine nitrogen of one arm. It is suggested that these hydrogen bonds could be formed only when the pyridine nitrogen atoms of the two other arms are deprotonated.

Complexation. Ferric O-TRENSEX Complexes. The large spectral change observed in the spectrophotometric titration of the ferric O-TRENSEX complex in acidic media is indicative of a change in the coordination of iron with the ligand. At $pH > 2$, the spectrum of the species is very similar to that of the tris(8-hydroxyquinoline-5-sulfonato)iron(III) complex (tris-oxinate coordination) ($\lambda_{max} = 450$ nm, $\epsilon = 5000$ M⁻¹ cm⁻¹, and $\lambda_{max} = 575$ nm, $\epsilon = 5100$ M⁻¹ cm⁻¹)²⁰ in which the iron is hexacoordinated to the three bidentate molecules through the phenolic oxygen atoms and the pyridine nitrogen atoms. Since the absorption coefficients of these bands are too large for a d-d transition, they are likely due to ligand-to-metal charge transfer (LMCT). The band at 443 nm is assigned to O → Fe^{III} charge transfer by comparison with other phenolate or catecholate complexes. It can thus be assumed that the band at 595 nm is of the N_{pyr} → Fe^{III} type. This band disappears in the spectrum of the FeLH₅²⁺ complex whereas the band at 440 nm is slightly shifted to lower energy (435 nm) with significant increase of the absorption coefficient (8200 M⁻¹ cm⁻¹). The change in the absorption spectrum can be interpreted by a change in the coordination sphere of the ferric ion. This suggests that N_{pyr} → Fe^{III} bonding is replaced by O → Fe^{III} bonding.

The infrared spectra provide additional information on the mode of bonding between the ferric ion and the ligand in the orange FeLH₅²⁺ and in the green FeL³⁻ complexes. The carbonyl band of FeL³⁻ appears at the same frequency (1650–1610 cm⁻¹) as in the free ligand. However, the carbonyl band of FeLH₅²⁺ is shifted to lower frequency (1630–1595 cm⁻¹) than the band of the free ligand. Such a lowering of the carbonyl absorption indicates a coordination of the carbonyl oxygen atom to the iron, as already observed for catecholate ferric complexes.³⁸ Furthermore, the spectrum of FeLH₅²⁺ contains an absorption at 1360 cm⁻¹ tentatively assigned to a free OH deformation which is absent from the spectrum of FeL³⁻. We are thus led to propose that, in the FeLH₅²⁺ complex, two arms of the ligand are coordinated to Fe(III) through a "salicylate" mode of coordination, the third one being free as depicted as

follows (L = H₂O; amide NH, quinoline ring, and SO₃⁻ omitted for clarity):



This structure is consistent with the proton stoichiometry of the complex. Furthermore, a tris(salicylate) complex must presumably be unfavorable in relation to high strain in the ligand backbone. The four-proton step deprotonation for the FeLH₅²⁺/FeLH²⁻ equilibrium is thus assumed to occur via a shift from a bis(salicylate) to a bis(oxinate) coordination (pyridine nitrogen and hydroxyl oxygen atoms) and the formation of an oxinate coordination with the free arm giving rise to a tris(oxinate) coordination of Fe(III) as deduced from the electronic spectrum. Finally, the deprotonation for the FeLH²⁻/FeL³⁻ equilibrium ($pK = 5.60$) is attributed to the tertiary amine, in agreement with the small change of the electronic spectrum at $pH > 2$. In accordance with the UV-vis and IR spectra of the ferric O-TRENSEX complex, the ¹H and ¹³C NMR spectra of ²H₂O solution of Ga^{III} and O-TRENSEX support the formation of two structurally different complexes depending on the pH. At low pH the well-resolved NMR spectrum is attributed to a protonated complex with three arms of the ligand magnetically nonequivalent. This appears consistent with two coordinated arms and one free arm. The assignment of the five protons to each arm is not discussed in this paper. However, NMR does not allow one to deduce the type of bonding between Ga(III) and the ligand. At higher pH, the ¹H NMR spectrum attributed to the deprotonated GaL³⁻ complex is consistent with a 3-fold symmetry of the ligand around the metal ion. Since 8-hydroxyquinoline is a nonsymmetrical bidentate ligand, meridional and facial isomers GaL³⁻ (or FeL³⁻) complex can exist. The ¹H NMR spectrum suggests the formation of the facial isomer since the three arms of the tripodal ligand are magnetically equivalent as expected for a facial isomer (3-fold symmetry). Interestingly, the spectra recorded for solutions containing a mixture of the two complexes show that these two species are in slow exchange on the NMR time scale.

In order to compare the Fe(III) complexation efficiency of O-TRENSEX with other iron chelators, the pFe value has been calculated under given ligand and metal concentration and for various pH values over the range 3–10. The corresponding pFe = f(pH) plot is presented in Figure 13 together with the plots calculated for other tripodal or reference ligands. In addition, the pFe values at physiological pH (7.4) are reported in Table 2. According to these values, O-TRENSEX is the strongest synthetic iron chelating agent over the pH range 3–8. At $pH > 8$, the pFe values of catecholate ligands are higher than those of O-TRENSEX, in relation to the higher pK_a .

Interestingly, the ligand N-TRENSEX has been found to be significantly less efficient than O-TRENSEX: the pFe value is about 7 orders of magnitude lower than that for O-TRENSEX. The explanation of the higher iron-sequestering properties of O-TRENSEX versus N-TRENSEX may reside in the hydrogen-bonding network available in the free ligand and in the complex. Indeed, hydrogen bonding has been claimed to play a significant role in the preorganization of the ligand for iron binding,^{39,40}

(38) Harris, W. R.; Raymond, K. N. *J. Am. Chem. Soc.* **1979**, *101*, 6534–6541

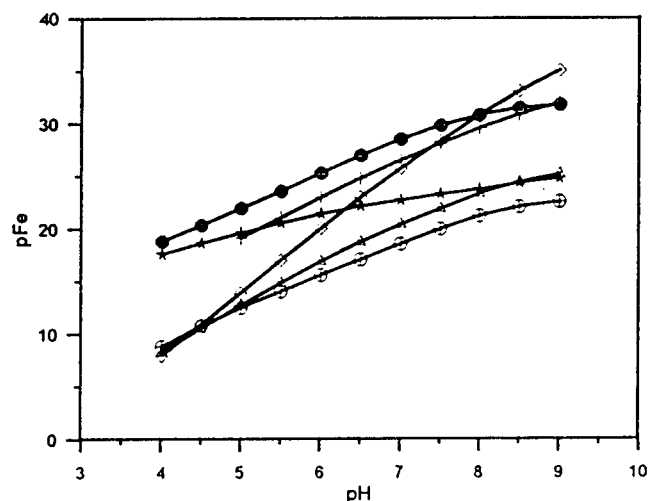


Figure 13. Plot of pFe vs pH for various tripodal ligands, EDTA, and sulfoxine. pFe was calculated for $[\text{Fe(III)}] = 1 \mu\text{M}$ and $[\text{L}] = 10 \mu\text{M}$ using the known constants of the tricatecholate TREN CAM⁹ (\diamond), trihydroxamate TRENDROX¹⁴ (+), EDTA²³ (*), and sulfoxine²⁰ (O), O-TRENDOX (\bullet), and N-TRENDOX (Δ).

especially to explain the very high affinity of enterobactin toward Fe(III).¹⁰ The amide group in N-TRENDOX is substituted ortho to the nitrogen of the quinoline ring while in O-TRENDOX it is substituted ortho to a phenolate oxygen. As a consequence, a salicylate coordination is favored for ferric O-TRENDOX in acidic media since hydrogen bonding between the carbonyl oxygen and the phenol "preorganizes" the ligand for this mode of bonding with the ion. This cannot occur with N-TRENDOX. Furthermore, as the coordination changes from a salicylate to an oxinate mode of bonding upon deprotonation of the complex, an amide conformational change is assumed to occur for the full complexation of the metal. So, hydrogen bonding of the amide and the corresponding preorganization of the complex must occur with O-TRENDOX. This is not the case with N-TRENDOX.

Electrochemistry. The potential of the ferric O-TRENDOX complex is more than 500 mV higher than that of hydroxamate siderophores (ferrioxamine B, $-0.468 \text{ V/NHE}^{41}$) and more than 800 mV higher than that of the catecholate siderophore enterobactin ($-0.750 \text{ V/NHE}^{42}$) and of the tricatecholate TREN CAM (-1.04 V/NHE^9). This indicates the lower selectivity of O-TRENDOX for ferric ion vs ferrous ion compared to the catecholate and hydroxamate ligands. As a consequence, the stability constant of the ferrous O-TRENDOX complex ($\log \beta_{110} = 19.3$) is significantly larger than that of the tricatecholate TREN CAM ($\log \beta_{110} = 12.6$) and of ferrioxamine B ($\log \beta_{110} = 9.5$) but lower than that of enterobactin ($\log \beta_{110} = 22.2$) owing to an exceptionally high stability constant for its ferric complex. Furthermore, the value of the reduction potential of the ferric O-TRENDOX indicates that the Fenton reaction is thermodynamically allowed. Nevertheless, we have shown that the ferrous complex is unable to promote the Fenton reaction owing to the kinetic barrier.²² This property makes O-TRENDOX relevant for biological applications.

Formation Kinetics. The formation reaction of the Fe(III)–O-TRENDOX complex in acidic medium has been found to

occur in one rate-limiting step involving the hydrolyzed ferric species $[\text{Fe}(\text{H}_2\text{O})_5\text{OH}]^{2+}$ and the fully protonated form of O-TRENDOX LH_7^+ and to lead to the FeLH_6^{3+} species. The value of the rate constant k_1 ($789 \text{ s}^{-1} \text{ M}^{-1}$) is slightly higher than that of sulfoxine⁴³ ($485 \text{ s}^{-1} \text{ M}^{-1}$, evaluated at 25°C from published values determined over the temperature range $35\text{--}45^\circ\text{C}$ at $I = 1 \text{ M}$). This result indicates that there is no steric hindrance due to the "TREN backbone" in the rate-determining step. Furthermore, the value of k_1 is in the same order of magnitude than those determined for various hydroxamate^{44,45} ($670\text{--}4300 \text{ s}^{-1} \text{ M}^{-1}$) and catecholate complexes^{46–48} ($1700\text{--}3300 \text{ s}^{-1} \text{ M}^{-1}$). In addition, the value of k_1 is very close to those determined for sulfonated 2,2'-dihydroxybiphenyl tripodal ligands¹⁷ ($485\text{--}821 \text{ s}^{-1} \text{ M}^{-1}$ at $I = 0.5 \text{ M}$). The rate constant k_1 is found to be slightly dependent on the structure of the ligand. This is interpreted by a dissociative Eigen–Wilkins mechanism⁴⁹ with a fast formation step of an outer-sphere complex (K_{os}) followed by a rate-limiting step involving the water substitution of the monohydroxylated Fe(III) species (k_{ex}):

$$k_1 = K_{\text{os}} k_{\text{ex}}$$

A mechanism can be proposed taking into account two structural features of the ligand O-TRENDOX: (i) The positively charged pyridine nitrogen site induces a repulsive effect on the incoming hydrated ferric species. (ii) The sulfonate group in the 5-position appears to be more favorable for ion-pairing in the precursor complex. Hence, it is suggested that initial bonding of the hydrated ferric ion proceeds through a coordination with the carbonyl oxygen atom followed by a rapid ring-closure with the phenolate oxygen to form a six-membered ring ("salicylate coordination"). The formation of the FeLH_5^{2+} species, as deduced from the equilibrium studies, is thus assumed to occur through a rapid salicylate type coordination with a second arm of the ligand.

Acid Hydrolysis Kinetics. The proposed protonation mechanism of the ferric O-TRENDOX complex (FeLH^{3-}) in acidic medium is depicted in Figure 14. On the basis of the kinetic results, a four stage mechanism has been proposed, corresponding to a partial dechelation at the iron center followed by a shift to a bis(salicylate) coordination and involving four intermediates. The structure of each intermediate is supported by the visible absorption spectrum.

Stage 1 has been found to occur very fast and to involve two protons. The spectrum of the intermediate kinetic species FeLH_3 , at the end of this stage (Figure 10a), is the same as the spectrum of the FeLH^{2-} complex, but with lower absorption coefficient at 595 nm ($\epsilon_1 = 3200 \text{ M}^{-1} \text{ cm}^{-1}$). It is similar to the spectrum of the Fe(III) bis(oxinate) complex.²⁰ This result is in favor of the removal of one arm from the inner coordination sphere of the Fe(III) center, leading to a bis(oxinate) mode of coordination, with the accompanying replacement by coordinated water molecules. Stage 2 has been found to be one-proton dependent and to lead to a decrease of the absorbance at 595 nm ($\epsilon_2 = 2000 \text{ M}^{-1} \text{ cm}^{-1}$) and a small increase at 443 nm (Figure 10b). Since the band at 595 nm has been attributed to

(43) Das, A. K. *Bull. Chem. Soc. Jpn.* **1992**, *65*, 2205–2210.

(44) Monzyk, B.; Crumbliss, A. L. *J. Am. Chem. Soc.* **1979**, *101*, 6203–6213.

(45) Brink, C. P.; Crumbliss, A. L. *Inorg. Chem.* **1984**, *23*, 4708–4718.

(46) Mentasti, E.; Pelizzetti, E. J. *J. Chem. Soc., Dalton Trans.* **1973**, 2605–2608.

(47) Mentasti, E.; Pelizzetti, E. J.; Saini, G. *J. Inorg. Nucl. Chem.* **1976**, *38*, 785–788.

(48) Xu, J.; Jordan, R. B. *Inorg. Chem.* **1988**, *27*, 1502–1507.

(49) Eigen, M.; Wilkins, R. G. *Mechanism of Inorganic Reactions. Adv. Chem. Ser.* **1965**, No. 49, 55–67.

(39) Garrett, T. M.; Cass, M. E.; Raymond, K. N. *J. Coord. Chem.* **1992**, *25*, 241–253.

(40) Shanzer, A.; Libman, J.; Lifson, S. *Pure Appl. Chem.* **1992**, *64*, 1421–1435.

(41) Wawrousek, E. F.; McArdle, J. V. *J. Inorg. Biochem.* **1982**, *17*, 169–183.

(42) Lee, C. W.; Ecker, D. J.; Raymond, K. N. *J. Am. Chem. Soc.* **1985**, *107*, 6920–6923.

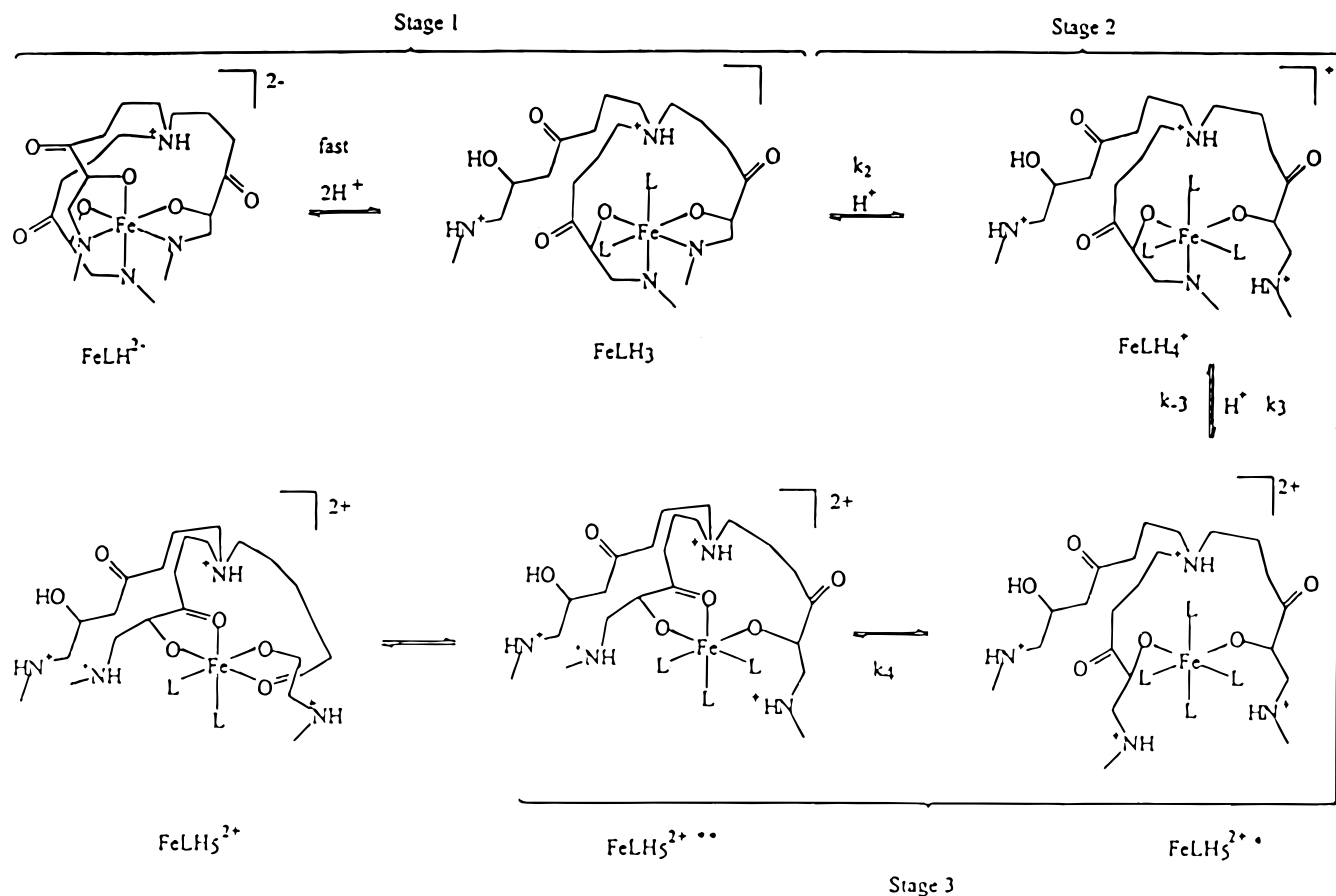


Figure 14. Proposed mechanism for the acid hydrolysis of the FeLH_2^- complex ($\text{L} = \text{H}_2\text{O}$; amide NH , quinoline rings, and SO_3^- omitted for clarity).

a $\text{Npyr} \rightarrow \text{Fe}$ ligand to metal charge transfer, it is reasonable to suppose that this stage is associated with the proton-assisted cleavage of a $\text{Fe}-\text{Npyr}$ bond and substitution by H_2O giving a tridentate bonded complex. Stage 3 involves H^+ -dependent equilibrium 17 followed by H^+ -independent reaction 18.

The equilibrium reaction rates are faster than the late reaction. The spectral change associated with reaction 17 is characterized by a very small variation of the absorbance at 443 nm and a decrease at 595 nm (see Figure 9). This suggests the proton-assisted cleavage of the third $\text{Fe}-\text{Npyr}$, as in stage 2, leading to formation of a bidentate intermediate. The increase of absorbance at 443 nm (Figure 10c) associated with reaction 18 can be explained by formation of a $\text{Fe}-\text{carbonyl}$ oxygen atom bond. It requires an exchange of a water molecule, giving rise to a tridentate intermediate involving coordination with three oxygen atoms. Stage 4 is characterized by a large increase of the absorbance at 443 nm suggesting the formation of a second $\text{Fe}-\text{carbonyl}$ oxygen coordination.

To our knowledge, there is no example of acid hydrolysis kinetics of ferric complexes with tripodal hexadentate ligands. Nevertheless, it would be instructive to compare the dissociation rate constants of the $\text{Fe(III)}-\text{O-TRENSEX}$ system with some literature data. Numerous data are available for the dissociation of the extensively studied ferrioxamine B,^{50,51} as well as $\text{Fe(III)}-\text{dihydroxamic acid}$ complexes⁵² and pyoverdin.⁵³ A step by step dissociation mechanism has been proposed for all of

these complexes with linear ligands, involving the successive protonations of the coordination sites. This process results in the unwrapping of the linear ligands and leads to the total dechelation of the metal. The values of the rate constants of stages 1–3 in the acid hydrolysis kinetics of the $\text{Fe(III)}-\text{O-TRENSEX}$ system can be compared with literature data since they characterize the dissociation of coordination bonds. The comparison shows that the dissociation of the first bidentate group (stage 1)⁵⁴ is significantly slower for hydroxamate type coordination in ferrioxamine B (290 or $380 \text{ M}^{-1} \text{ s}^{-1}$)^{50,51} and for catecholate type coordination in pyoverdin⁵³ ($1800 \text{ M}^{-1} \text{ s}^{-1}$) than for sulfoxinate type coordination in O-TRENSEX . This process is very fast since steric strain in the ligand may increase the rate of $\text{Fe}-\text{Npyr}$ and $\text{Fe}-\text{O}$ cleavage. An other possible explanation for the high kinetic lability of the hexacoordinated complex may be invoked by considering the solvent rearrangement resulting from dissociation of one sulfoxine group, as already supported for hydroxamate dissociation.⁵⁵ An association by hydrogen bonds may be envisioned in the tetradentate complex FeLH_3 between the water molecules coordinated to Fe(III) and the free sulfoxine moiety, probably through oxygen atoms. This results in a small motion of the arm as it dissociates from the Fe(III) and a slight solvent rearrangement. So, the hexadentate \rightleftharpoons tetradentate equilibrium may be a facile process. The rate constant k_2 related to the tetradentate \rightarrow tridentate reaction can be compared to the values obtained for a similar

(50) Monzyk, B.; Crumbliss, A. L. *J. Am. Chem. Soc.* **1982**, *104*, 4921–4929.

(51) Birus, M.; Bradic, Z.; Krznaric, G.; Kujundzic, N.; Pribanic, M.; Wilkins, P. C.; Wilkins, R. G. *Inorg. Chem.* **1987**, *26*, 1000–1005.

(52) Caudle, M. T.; Cogswell, L. P.; Crumbliss, A. L. *Inorg. Chem.* **1994**, *33*, 4759–4773.

(53) Albrecht-Gary, A.-M.; Blanc, S.; Rochel, N.; Ocaktan, A. Z.; Abdallah, M. A. *Inorg. Chem.* **1994**, *33*, 6391–6402.

(54) A lower limit for the dissociation rate constant related to stage 1 (reaction 13) can be estimated to approximately $5000 \text{ s}^{-1} \text{ M}^{-1}$ on the basis of a 2–6 ms reaction half-time for $[\text{H}^+] = 0.1\text{--}0.02 \text{ M}$.

(55) Caudle, M. T.; Crumbliss, A. L. *Inorg. Chem.* **1994**, *33*, 4077–4085.

process involving dissociation of a tetradentate into a tridentate complex which was observed in the acid hydrolysis of ferrioxamine B⁵⁰ and of Fe^{III}-dihydroxamic acid complexes.⁵² The values, over the range 10–17 M⁻¹ s⁻¹, are significantly lower than the value (643 M⁻¹ s⁻¹) obtained for Fe^{III}-O-TRENSEX, suggesting a high kinetic lability of the Fe–N_{pyr} bonds. As previously invoked, this can be related to a slight solvent rearrangement resulting from “half-opened” chelation.

The rate constants $k_2 = 643 \text{ M}^{-1} \text{ s}^{-1}$ and $k_3 = 5.7 \text{ M}^{-1} \text{ s}^{-1}$ are decreased as expected in a stepwise dissociation. The fact that k_3 is decreased by a factor of 113 with respect to k_2 can be best explained by considering the repulsive effect of the positive charge on the pyridine nitrogen atoms on the incoming proton which is necessary for dissociation. Indeed, the two successive ring openings of the oxinate chelation probably imply a small solvent rearrangement. Therefore, the Fe–N_{pyr} bond cleavage rates from analysis of stage 1 (too fast to be measured), stage 2 (k_2), and stage 3 (k_3) are decreased from the complex with three Fe–N_{pyr} bonds to the complex with no Fe–N_{pyr} bond as observed in a dissociation mechanism.⁵⁶

The last step of the mechanism has been tentatively assigned to the formation of coordination with two carbonyl oxygen atoms on the basis of the UV–visible spectra. We were able to determine the rate constant ($k_4 = 0.26 \text{ s}^{-1}$) corresponding to the first carbonyl oxygen coordination. The value has to be related to the rates of rotation around the C–C and C–N bonds of the chain connecting the central nitrogen to the sulfoxine moiety. One might expect that the rate of rotation around the C–N bond of the amide group would be the slowest owing to its partial double-bond character. The formation of the second carbonyl coordination occurs over a 20–200 s time scale. The nonexponential behavior of this process is hard to interpret. We suppose that the rearrangement necessary to coordination is hindered by the strains in the complex.

Finally, the picture that emerges from the mechanism of the hydrolysis of the Fe^{III}-O-TRENSEX complex in highly acidic medium is that the stepwise protonation reactions lead to a partial unwrapping of the hexadentate ligand. This results in a labile structure forming a tight cavity around the ferric ion. The positive charges on the pyridine nitrogen atoms are assumed to repel incoming H⁺ necessary for dissociation. A shift to a bis-(salicylate) coordination is thus favored with respect to the release of Fe(III).

(56) Birus, M.; Kujundzic, N.; Pribanic, M. *Prog. React. Kinet.* **1993**, *18*, 171–271.

Conclusion

The present work has shown that the tripodal ligand O-TRENSEX possessing three bidentate oxine subunits is a very strong chelator for Fe(III) over a large range of pH from acidic to basic medium. Our results confirm that the tripodal structure is well adapted for strong hexadentate coordination. The interesting feature of O-TRENSEX is that the amide connection in the ortho position with respect to the hydroxyl group favors an initial strong coordination of the salicylate type, which probably “preorganizes” the ligand for a full complexation of the metal by the three oxinate ligands. This is in contrast with the behavior of the ligand N-TRENSEX with an amide connection in the ortho position with respect to the pyridine nitrogen. This ligand is characterized by a poor affinity for Fe(III). The remarkable property of O-TRENSEX is its high complexing ability for both the ferric and ferrous ion redox states, contrary to the catecholate and hydroxamate ligands. The redox potential of 0.087 V vs NHE is more than 0.4 and 0.8 V higher than that of the hydroxamate and catecholate ferric complexes, respectively. The kinetic study of the acid hydrolysis of the Fe^{III}-O-TRENSEX complex provides additional information on the change of coordination in relation to the protonation state of the complex. Furthermore, the proposed mechanism for the acid hydrolysis shows that the complex has one labile arm and two relatively labile Fe–N_{pyr} coordination bonds. This feature is important in view of ligand interchange process. So, attack by a competing ligand would be expected to form a ternary complex which may be kinetically labile. The lability of some coordination sites is an important parameter for the release of iron by siderophores to microorganisms. This lability can occur through ligand exchange. O-TRENSEX has been found to be efficient in the iron nutrition of plants.²² Our kinetic data provide an element for understanding this efficiency. Further investigations on ligand exchange are now in progress.

Acknowledgment. We are grateful to Dr. Eric Saint Aman (LEOPR, Grenoble, France) for his help on electrochemical measurements and to Dr. Claude Dumont (LEDSS, Grenoble, France) for the automation of potentiometric titration. We thank Professor A. L. Crumbliss (Durham, NC) and Dr. A.-M. Albrecht-Gary (Strasbourg, France) for very helpful discussions.